

# HYBRID CONTROL DESIGN FOR A ROBOT MANIPULATOR IN A SHIELD TUNNELING MACHINE

Jelmer Braaksma, Ben Klaassens, Robert Babuška  
*Delft Center for Systems and Control, Delft University of Technology  
Mekelweg 2, 2628 CD Delft, the Netherlands*

Cees de Keizer  
*IHC Systems B.V., P.O. Box 41, 3360 AA Sliedrecht, the Netherlands*

**Keywords:** Robotic manipulator, shield tunneling, hybrid control, collision, environment model, feedback linearization.

**Abstract:** In a novel shield tunneling method, the tunnel lining is produced by an extrusion process with continuous shield advance. A robotic manipulator is used to build the tunnel supporting formwork, consisting of rings of steel segments. As the shield of the tunnel-boring machine advances, concrete is continuously injected in the space between the formwork and the surrounding soil. This technology requires a fully automated manipulator, since potential human errors may jeopardize the continuity of the tunneling process. Moreover, the environment is hazardous for human operators. The manipulator has a linked structure with seven degrees of freedom and it is equipped with a head that can clamp the formwork segment. To design and test the controller, a dynamic model of the manipulator and its environment was first developed. Then, a feedback-linearizing hybrid position-force controller was designed. The design was validated through simulation in Matlab/Simulink. Virtual reality visualization was used to demonstrate the compliance properties of the controlled system.

## 1 INTRODUCTION

With conventional shield tunnel boring machines (TBM), the tunnel lining is built of pre-fabricated concrete segments (Tanaka, 1995; K. Kosuge et al., 1996). These segments must be transported from the factory to the construction site, which requires considerable logistics effort. Delays in delivery and damage of the segments during their transport are not uncommon.

To improve the process, IHC Tunneling Systems are developing a novel shield tunneling method in which the tunnel lining is produced by extruding concrete in the space between the drilled hole and the supporting steel formwork. This formwork is built of rings, each consisting of eight segments.

The main functions of the formwork are: i) support the extruded concrete tunnel lining until it is hardened and becomes self-supporting, ii) provide the thrust force to the TBM shield which actually excavates the tunnel. The thrust is supplied by 16 individually controlled hydraulic thrust cylinders, evenly spread around the shield's circumference.

A robotic manipulator (erector) is used to place the segments at the desired position. The erector is a linked robot mounted such that it can rotate around

the TBM spine, see Fig. 1. It is equipped with a head that clamps the segment and picks it up from the conveyor. At the back end of the TBM, the concrete is already hardened and the formwork can be dismantled by a similar manipulator (derector). The segments are cleaned and inspected for possible damage before they can be transported to the front end of the TBM and re-used.

As in the proposed method the tunnel-boring process is continuous (maximum speed of 2 m/h), the segments have to be placed within a limited time interval, and simultaneously with the TBM forward movement. To comply with the stringent timing requirements and to ensure the continuity of the boring process, the erector must be controlled automatically (as opposed to the current practice of using operator-controlled manipulators). By automating the process, the probability of a human error is limited and also the hazard for the operator is considerably reduced.

The controller of the erector must guarantee stable and safe operation in three different modes (Fig. 2):

1. The segment is in free space and the main task is to bring it close to the desired position.
2. The segment is in contact with the hydraulic thrust cylinders which push it toward the already placed formwork ring.

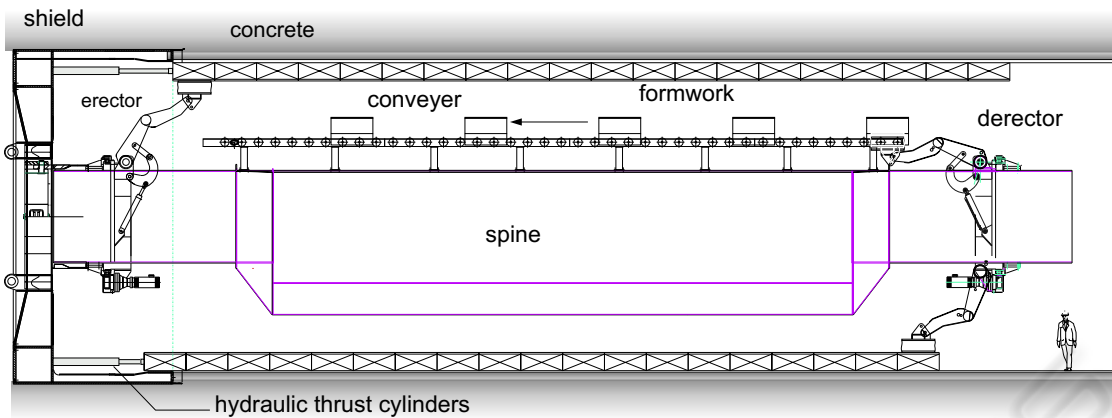


Figure 1: Cross-section of the shield tunneling machine. Two working configurations of the derector are shown.

3. The segment is in contact with the hydraulic thrust cylinders and the formwork ring. The force delivered by the thrust cylinders will align the segment in the desired position.

While the first mode is characterized by traditional trajectory-following control, the latter two modes require compliant control, capable of limiting the contact forces and correcting a possible mis-alignment due to a different orientation of the segment and the already placed ring. Note that no absolute measurement of the segment position is available, it can only be indirectly derived from the measurements of the individual angles of the manipulator links.

To analyze the process and to design the control system, a detailed dynamic model of the erector has been developed. This model includes collision models for operation modes 2 and 3. A hybrid control scheme is then applied to control certain DOFs by a position control law and the remaining ones by a force control law. Input-output feedback linearization is applied in the joint space coordinates. Simulation results are reported.

## 2 MODELING

The mathematical model consists of three parts: the manipulator, the environment and the hydraulic thrust cylinders. This section describes these elements one by one.

### 2.1 Manipulator model

The erector was designed as a linked structure with three arms and a fine-positioning head, see Fig. 3. The first arm is attached to the base ring (body0) that can rotate around the spine. This ring is actuated by an electric motor. The arms are actuated by hydraulic

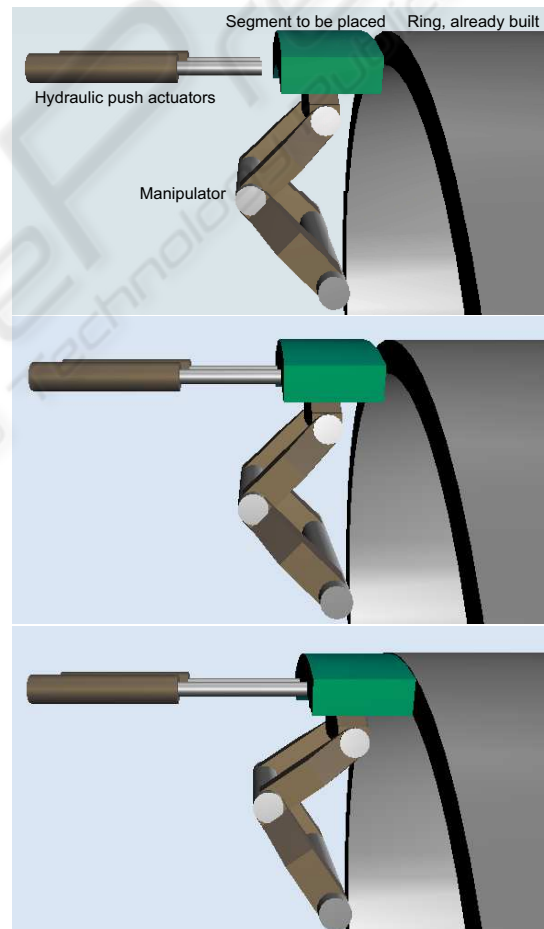


Figure 2: The erector manipulates segments in three different modes: in free space (top), in contact with the hydraulic thrust cylinders (middle), in contact with the trust cylinders and the segment ring (bottom).

actuators (not modeled here). At the top of the third arm (body3), the head is attached, which has three degrees of freedom (DOF). The entire manipulator has seven DOF ( $q_0$  to  $q_6$ ) in total.

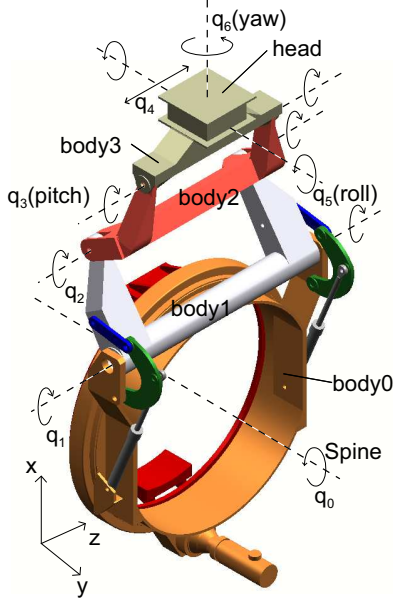


Figure 3: The structure and the corresponding degrees of freedom of the erector.

The bodies are assumed rigid bodies and the DOF in body0 is not taken into account. This is justified, as the rotation around the spine is fixed during the positioning of the head. Angle  $q_0$  is still an input to the model, fixed to a value between 0 and  $2\pi$  rad. The control inputs of the robot are assumed to be perfect torque/force generators in the joints.

The dynamic equation for the manipulator is:

$$D(\mathbf{q})\ddot{\mathbf{q}} + C(\mathbf{q}, \dot{\mathbf{q}})\dot{\mathbf{q}} + F_v\dot{\mathbf{q}} + \phi(\mathbf{q}) = \boldsymbol{\tau} - J_0^{b4}(\mathbf{q})^T \mathbf{f} \quad (1)$$

where  $\mathbf{f}$  is the vector of contact forces between the hydraulic thrust cylinders and the segment plus the contact forces between the segment and the ring. The matrix  $D(\mathbf{q})$  is the inertia matrix,  $C(\mathbf{q}, \dot{\mathbf{q}})$  is the Coriolis and centrifugal matrix,  $F_v$  is the friction matrix and  $\phi(\mathbf{q})$  is the gravity vector.  $J_0^{b4}$  is the Jacobian from frame  $b4$  to frame 0, and  $q$  is the vector of the joint angles. The manipulator is actuated with the torque/force vector  $\boldsymbol{\tau}$ .

## 2.2 Environment model

The environment consists of the segment ring (Fig. 4). An accurate environment model, very important to the contact tasks in robotics, is usually difficult to obtain in an analytic form. In the literature, usually a simplified linear model is used (Vukobratović,



Figure 4: Two consecutive rings of the formwork. Each ring consists of eight segments.

1994). The environment is modeled as a mass-spring-damper-system. The surface of the segment's side is considered flat and only the normal force acting on the side of the segment is taken into account. Tangential friction forces are neglected. The collision detection is implemented with the following smooth switching function

$$g(x) = \frac{1}{\pi} \text{atan}(\alpha(x - x_e)) + \frac{1}{2} \quad (2)$$

where  $\alpha$  is the steepness of the function,  $x$  is the position of the segment and  $x_e$  is the position of the environment. The environment force is described by the following equation:

$$\mathbf{f}_e = g(x)(K_e(x - x_e) + D_e(\dot{x} - \dot{x}_e)) \quad (3)$$

For stationary environments, equation (3) can be simplified by taking  $\dot{x}_e = 0$ .  $K_e$  is the stiffness and  $D_e$  is the damping.

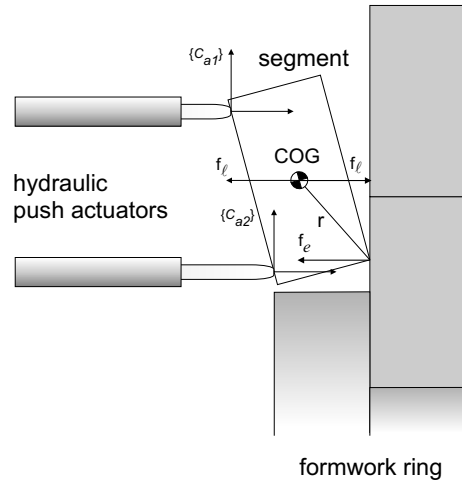


Figure 5: Decomposition of contact force  $\mathbf{f}_e$ .

In the Cartesian space, the dynamic behavior depends on the direction vector of the force and the location of the collision. Fig. 5 shows an unaligned collision of the segment with the formwork ring. In this

figure, a transformation is applied, which decomposes a force  $\mathbf{f}_e$  into a force  $\mathbf{f}_l$  and torque  $\boldsymbol{\tau}$  acting on the center of gravity (COG). The following formulas can be applied.

$$\mathbf{f}_l = \mathbf{f}_e \quad (4)$$

$$\boldsymbol{\tau} = \mathbf{r} \times \mathbf{f}_e \quad (5)$$

where  $\mathbf{r}$  points to the place where the force acts. The above derivation is valid for a body moving in free space. The transformation of the force and torque to the joint torque is achieved using the principle of virtual work, see (Spong and Vidyasagar, 1989). The following formula for the joint torques can be derived

$$\boldsymbol{\tau}_e = J_0(\mathbf{q})^T \begin{bmatrix} \mathbf{R}_0^{b4} & \mathbf{0} \\ \mathbf{0} & \mathbf{R}_0^{b4} \end{bmatrix} \mathbf{f} \quad \text{with } \mathbf{f} = \begin{bmatrix} \mathbf{f}_l \\ \boldsymbol{\tau} \end{bmatrix} \quad (6)$$

where  $\mathbf{R}_0^{b4}$  transforms the force expressed in the segment body frame to the base frame,  $J_0(\mathbf{q})$  is the Jacobian which transforms the joint speeds to the linear/rotational speeds in the base frame and  $\boldsymbol{\tau}_e$  is a vector with joint torques/forces.

### 2.3 Hydraulic thrust cylinders

The model consists of a collision model and a hydraulic model. The collision model must detect the collision between the hydraulic thrust cylinders and the formwork ring, which means that the model must detect whether the tips are contacting the segment body (body4). If there is a collision, the magnitude of the force can be calculated with the scheme explained in Section 2.2.

The shape of a segment is illustrated in Fig. 6. The segment (body4) is a part of a hollow cylinder. For a controlled collision, the  $y$  coordinate of tip of the hydraulic thrust cylinders must be between the inner radius  $r_1$  and the outer radius  $r_2$ , and within the range  $\varphi$ , see Fig. 6. The kinematic transformation of two hydraulic thrust cylinders tips to the  $C_{b4}$  frame is used to detect collision.

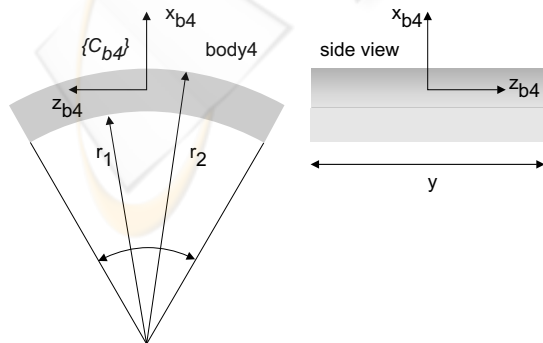


Figure 6: The dimensions of the segment (body4).

When the actuators come into contact with the segment, this will result in a force and torque as explained in Fig. 5. Only the normal force acting on the segment is simulated. The error between the segment and the thrust cylinders is at most 3 degrees, satisfying the assumption to neglect the tangential force. The force and torque in the  $C_{b4}$  frame, are calculated with the following equations. Let  $H_{a1}^{b4}$  and  $H_{a2}^{b4}$  be the homogeneous transformations from the thrust cylinder frames ( $C_{a1}$ ,  $C_{a2}$ ) to  $C_{b4}$ . The two force and torque vectors can be calculated as follows

$$\mathbf{f}_{a1} = |f_{a1}|[0 \ 1 \ 0]^T \quad \mathbf{r}_{a1} = (H_{b4}^{a1}[0 \ 0 \ 0 \ 1]^T)_{123} \quad (7)$$

$$\boldsymbol{\tau}_{a1} = \mathbf{r}_{a1} \times \mathbf{f}_{a1}$$

$$\mathbf{f}_{a2} = |f_{a2}|[0 \ 1 \ 0]^T \quad \mathbf{r}_{a2} = (H_{b4}^{a2}[0 \ 0 \ 0 \ 1]^T)_{123} \quad (8)$$

$$\boldsymbol{\tau}_{a2} = \mathbf{r}_{a2} \times \mathbf{f}_{a2}$$

where the subscript 123 refers to the first three elements. These forces and torques in the body frame can be transformed to the joint torques by means of the principle of virtual work (6).

### 3 HYBRID CONTROLLER

The manipulator in free space is position controlled, but when it is in contact with the environment, the lateral motion and rotation become constrained. When the segment is pushed by the hydraulic thrust cylinders, stable contact between the thrust cylinders and the segment is maintained by controlling the contact force (Fig. 7). When the segment comes into contact with the segment ring, it aligns to the desired orientation and position. During the transition between the modes it is required that the contact forces are limited. An impedance controller gives the manipulator the desired compliant behavior (Hogan, 1985).

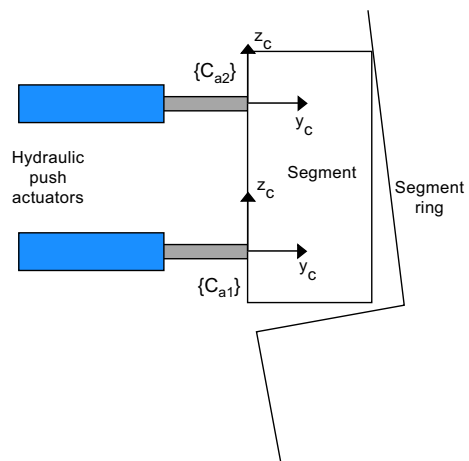


Figure 7: Top view of the segment.

A control scheme known as a hybrid position force controller of (Raibert and Craig, 1981) allows to specify for each DOF the type of control. The frame in which the segment is controlled is positioned such that the direction, in which the position is controlled, is perpendicular to the direction in which the force is controlled. This frame is called the constraint frame. In our case the constraint frame is aligned with the two thrust cylinder frames (see Fig. 7). In this situation, the yaw,  $y$ , and the pitch,  $z$ , DOFs are constrained. We choose for the  $y$  degree of freedom a force controller to assure contact. For the other position constrained degrees of freedom an impedance controller is chosen which guarantees compliant behavior.

The controller consists of four blocks: feedback linearization, transformation of sensor data (kinematics, Jacobian and coordinate transform), selection matrix and the controllers (see Fig. 8).

The coordinate-transform block transforms the data  $\mathbf{f}$ ,  $\mathbf{x}$ ,  $R$ ,  $\mathbf{v}$  and  $\boldsymbol{\omega}$  from the base frame to the constraint frame and vice versa, where  $\mathbf{f}$  is the measured force,  $\mathbf{x}$  is the position of the segment,  $R$  is the rotation matrix which defines the orientation of the segment,  $\mathbf{v}$  is the linear speed of the segment and  $\boldsymbol{\omega}$  is the angular speed of the segment. The inputs of the force controller are  $\mathbf{f}_d$  and  $\dot{\mathbf{f}}_d$ , which are the desired force and its derivative. The inputs of the position controller are  $\mathbf{x}_d$ ,  $\dot{\mathbf{x}}_d$  and  $\ddot{\mathbf{x}}_d$ , which are the desired position, velocity and acceleration respectively. The vector  $\mathbf{a}$  is the resolved acceleration vector and  $\boldsymbol{\tau}$  is the torque/force vector for the manipulator.

### 3.1 Feedback linearization

The following controller is used for feedback linearization (Siciliano and Villani, 1999)

$$\boldsymbol{\tau} = \hat{D}(\mathbf{q})\mathbf{u} + \hat{C}(\mathbf{q}, \dot{\mathbf{q}})\dot{\mathbf{q}} + \hat{F}_v\dot{\mathbf{q}} + \hat{\phi}(\mathbf{q}) + J_0^{b4}(\mathbf{q})^T \mathbf{f} \quad (9)$$

where  $\mathbf{u}$  is the new acceleration control input. Substituting (9) into (1) and assuming perfect modeling results in the following system

$$\ddot{\mathbf{q}} = \mathbf{u} \quad (10)$$

The goal of the controller is to control the manipulator in the constraint frame to its desired values.

The Jacobian transforms the joint velocities to the linear and rotational speeds. The Jacobian is given by

$$\begin{bmatrix} \mathbf{v}_0^{b4} \\ \boldsymbol{\omega}_0^{b4} \end{bmatrix} = J_0^{b4}(\mathbf{q})\dot{\mathbf{q}} \quad (11)$$

Differentiating (11) gives

$$\begin{bmatrix} \dot{\mathbf{v}}_0^{b4} \\ \dot{\boldsymbol{\omega}}_0^{b4} \end{bmatrix} = \ddot{\mathbf{x}} = J_0^{b4}(\mathbf{q})\ddot{\mathbf{q}} + \dot{J}_0^{b4}(\mathbf{q})\dot{\mathbf{q}} \quad (12)$$

which represents the relationship between the joint acceleration and the segment's linear and rotational speed. A new control input can now be chosen as

$$\mathbf{u} = (J_0^{b4}(\mathbf{q}))^{-1} \left( \mathbf{a} - \dot{J}_0^{b4}(\mathbf{q})\dot{\mathbf{q}} \right). \quad (13)$$

Substitute (13) into (10) and the result into (12), assuming perfect modeling and perfect force measurement, leads to the following total plant model

$$\ddot{\mathbf{x}} = \mathbf{a} = \mathbf{a}_p + \mathbf{a}_f \quad (14)$$

where  $\mathbf{a}$  is the resolved acceleration in the base frame and  $\mathbf{a}_p$ ,  $\mathbf{a}_f$  are the outputs of the position controller and force controller in the base frame. The vector  $\mathbf{a}_p$  can be partitioned into linear acceleration  $\mathbf{a}_l$  and angular acceleration  $\mathbf{a}_o$ . Likewise,  $\mathbf{a}_f$  can be partitioned into linear acceleration  $\mathbf{a}_{fl}$  and angular acceleration  $\mathbf{a}_{ft}$ :

$$\mathbf{a}_p = \begin{bmatrix} \mathbf{a}_l \\ \mathbf{a}_o \end{bmatrix} \quad \mathbf{a}_f = \begin{bmatrix} \mathbf{a}_{fl} \\ \mathbf{a}_{ft} \end{bmatrix}. \quad (15)$$

### 3.2 Transformation of sensor data

The different positions and speeds are measured in the joints of the manipulator. The force is measured using a force sensor, located in the manipulator head. To control the manipulator in Cartesian space these measurements must be transformed to a Cartesian frame. This is done with the kinematic matrix and the Jacobian matrix. The frame in which the manipulator is controlled is the constraint frame.

### 3.3 Selection matrix

The DOF for position control and for force control can be selected. This is done by multiplying the force/torque vector by a diagonal selection matrix  $S$  and the position/velocity vector by  $I - S$ , with  $I$  the identity matrix. For a DOF that is position controlled  $S_i = 0$  and for a force controlled DOF  $S_i = 1$ . For a manipulator moving in free space the selection matrix is a zero matrix, meaning position control.

To make sure that the switch between the two situations is in a controlled manner, the switch function of the selection matrix must be smooth. The time of switching is unknown, so the switch should be triggered by the contact force (Zhang et al., 2001).

$$\Phi_i(f_i) = \begin{cases} f_i - f_{ref1}^i, & \text{if } f_i \geq 0 \\ f_{ref2}^i - f_i, & \text{if } f_i < 0 \end{cases} \quad (16)$$

The smooth switch function can now be defined as

$$S_i = \begin{cases} 0, & \text{if } \Phi_i(f_i) < 0 \\ 1 - \text{sech}(\alpha\Phi_i(f_i)), & \text{otherwise} \end{cases} \quad (17)$$

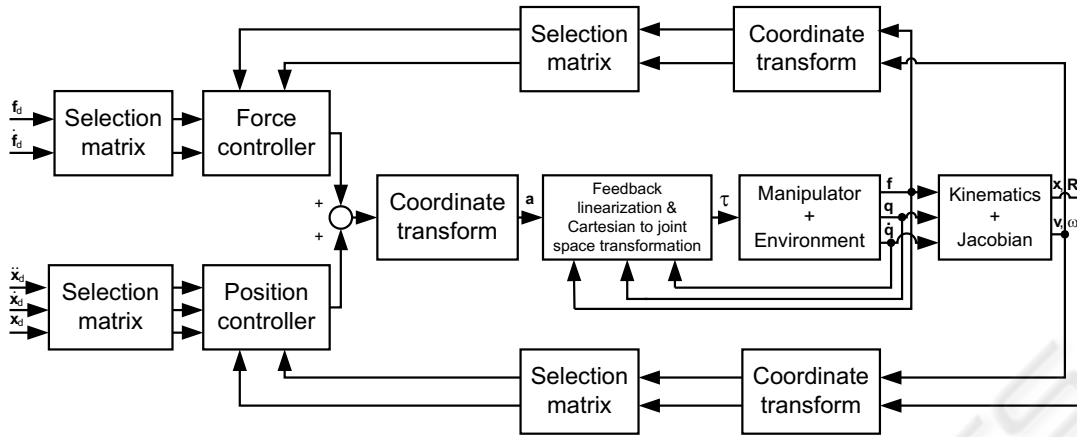


Figure 8: Block diagram of the hybrid position force controller.

with

$$\text{sech}(x) = \frac{2}{e^x + e^{-x}} \quad (18)$$

The value  $\alpha$  determines the steepness of the curve, and  $f_{ref1}^i$ ,  $f_{ref2}^i$  are the upper and lower threshold values respectively. The steepness  $\alpha$  should be chosen such that the  $S_i = 1$ , when the desired contact force is reached. The force in the y DOF (in the constraint frame) is chosen to switch from position control to force/impedance control.

### 3.4 Position control

For the linear and decoupled system (14), the following control can be used in order to give the system the desired dynamics (Siciliano and Villani, 1999).

$$\mathbf{a}_l = \ddot{\mathbf{x}}_d + D_l(\dot{\mathbf{x}}_d - \dot{\mathbf{x}}) + P_l(\mathbf{x}_d - \mathbf{x}) \quad (19)$$

$$\mathbf{a}_o = \dot{\boldsymbol{\omega}}_d + D_o(\boldsymbol{\omega}_d - \boldsymbol{\omega}) + P_o R_{b_4}^c \epsilon_{b_4}^d \quad (20)$$

This is a PD controller for the position controlled DOF, where  $R_{b_4}^c$  transforms the quaternion error  $\epsilon_{b_4}^d$  from the  $C_{b_4}$  frame to the constraint frame. The matrices  $D_l$  and  $D_o$  are the diagonal damping matrices, and  $P_l$  and  $P_o$  are the proportional gain matrices. Substituting (19) and (20) into (14) assuming perfect modeling gives the total plant model

$$\ddot{\mathbf{x}} = \overline{S} \begin{bmatrix} \ddot{\mathbf{x}}_d + D_l(\dot{\mathbf{x}}_d - \dot{\mathbf{x}}) + P_l(\mathbf{x}_d - \mathbf{x}) \\ \dot{\boldsymbol{\omega}}_d + D_o(\boldsymbol{\omega}_d - \boldsymbol{\omega}) + P_o R_2^e \epsilon_e^{de} \end{bmatrix} \quad (21)$$

### 3.5 Force control

The force controller has an inner position/orientation loop within the force loop. For the position loop, the following PD-controller is chosen (Siciliano and Villani, 1999).

$$\mathbf{a}_f = -D_f \dot{\mathbf{x}} + P_{fp}(\mathbf{x}_c - \mathbf{x}) \quad (22)$$

where  $\mathbf{x}_c - \mathbf{x}$  is the difference between  $\mathbf{x}_c$  the output of the force loop and the measured position/orientation  $\mathbf{x}$  and  $P_{fp}$  is the proportional matrix gain and  $D_f$  is damping gain. For the force loop a proportional-integral (PI) control is chosen

$$\mathbf{x}_c = P_{fp}^{-1} \left( P_f(\mathbf{f}_d - \mathbf{f}) + P_I \int_0^t (\mathbf{f}_d - \mathbf{f}) d\zeta \right) \quad (23)$$

where  $P_f$  is the proportional gain,  $P_I$  is the integral gain,  $\mathbf{f}_d$  is the desired force and  $\mathbf{f}$  is the measured force. The  $P_{fp}^{-1}$  in (23) has been introduced to make the resulting force and moment control action in (22) independent of the choice of the proportional gain on the position and orientation.

### 3.6 Impedance control

For the impedance controlled DOF the following control law can be chosen (Siciliano and Villani, 1999)

$$\mathbf{a}_f = \begin{bmatrix} \ddot{\mathbf{x}}_d + M_{li}^{-1}(D_{li}(\dot{\mathbf{x}}_d - \dot{\mathbf{x}}) + P_{li}(\mathbf{x}_d - \mathbf{x}) - \mathbf{f}_l) \\ \dot{\boldsymbol{\omega}}_d + M_{oi}^{-1}(D_{oi}(\boldsymbol{\omega}_d - \boldsymbol{\omega}) + P_{oi} R_{b_4}^c \epsilon_{b_4}^d - \mathbf{f}_t) \end{bmatrix} \quad (24)$$

with  $M_{li}$  and  $M_{oi}$  positive definite matrix gains, leading to

$$M_{li}(\ddot{\mathbf{x}}_d - \ddot{\mathbf{x}}) + D_{li}(\dot{\mathbf{x}}_d - \dot{\mathbf{x}}) + P_{li}(\mathbf{x}_d - \mathbf{x}) = \mathbf{f}_l \quad (25)$$

$$M_{oi}(\dot{\boldsymbol{\omega}}_d - \dot{\boldsymbol{\omega}}) + D_{oi}(\boldsymbol{\omega}_d - \boldsymbol{\omega}) + P_{oi} R_{b_4}^c \epsilon_{b_4}^d = \mathbf{f}_t \quad (26)$$

Equations (25) and (26) allow specifying the manipulator dynamics through the desired impedance, where the translational impedance is specified by  $M_{li}$ ,  $D_{li}$  and  $P_{li}$  and the rotational impedance is specified by  $M_{oi}$ ,  $D_{oi}$  and  $P_{oi}$ .

### 3.7 Simulation results

The rotation around the spine is fixed during fine positioning at  $q_0 = 0$ . The segment ring has a different orientation than the segment; it is rotated around the yaw axis by 0.05 radians. In order to take model uncertainties into account, errors are introduced in the model. For the dynamic parameters such as inertia an error of 10% is introduced and for length and positions an error of 1% is introduced. As it is impossible to simulate all combination of parameter errors, the errors are randomly chosen for every simulation.

In the position loop, the P-gain is chosen  $P_l = 10I$ . This corresponds with a natural frequency of 3.2 rad/s and for the D-gain  $D_l = 6.3I$  and this corresponds to a damping ratio of 1. For the pitch and roll axes the same gains  $P_o = 10I$  and  $D_o = 6.3$  are used. The desired force input is 500 N. The position loop in the force controller has also a P-gain of  $P_{fp} = 10I$  and a D-gain of  $D_f = 6.3I$ . The P-gain of the force controller is  $P_{fp} = 5 \cdot 10^{-3}I$  and the I-gain is set  $P_I = 5 \cdot 10^{-3}I$ . The parameters of the impedance-controlled DOFs are given by  $M_{li} = 100I$ ,  $D_{li} = 250I$  and  $P_{li} = 500I$  for the  $z$  DOF and  $M_{oi} = 300I$ ,  $D_{oi} = 50000I$  and  $P_{oi} = 100I$  for rotational DOF.

At  $t=0$  s the manipulator is in position control, and there is no contact between the segment and the environment. The thrust cylinders start moving and get in contact with the segment at  $t=4.8$  s. The manipulator switches to force/impedance control and moves further with the same speed as the hydraulic thrust cylinders (see Fig. 9). The  $y$  position of the environment is at  $y = 0.25$  m. When the segment contacts the environment at  $t = 8$  s, the segment aligns with the environment as shown in Fig. 10. This contact gives rise to a torque  $\tau_x$  of 800 Nm in the head, which is measured by the force sensor (Fig. 11). This torque is caused by the damping term in the impedance controller. The rotational speed is 0.0017 rad/s the damping term is 50000, the torque is then  $0.0017 \times 50000 = 833$  Nm.

The simulations are repeated 50 times, each time the parameters in the controller's internal model are chosen randomly. In Fig. 11 and Fig. 12, the measurements of the force sensor are plotted. The magnitude of the force in the  $y$  DOF is not influenced; the time of impact varies due to the parameter changes. The torque around the  $z$  axis is influenced by the parameter change.

## 4 CONCLUSIONS

A dynamic model of the manipulator and its environment has been successfully derived and implemented in Matlab/Simulink. The control requirements have

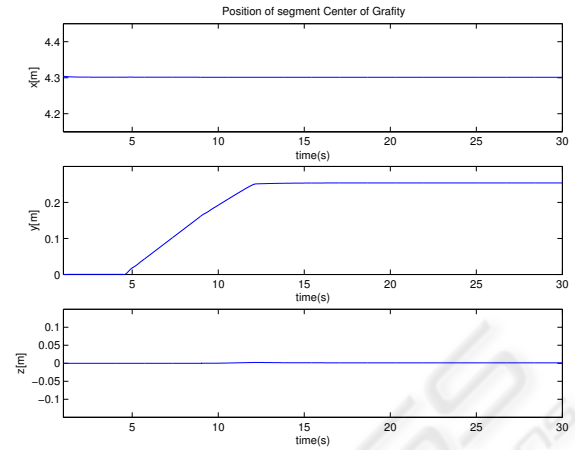


Figure 9: Position of the segment.

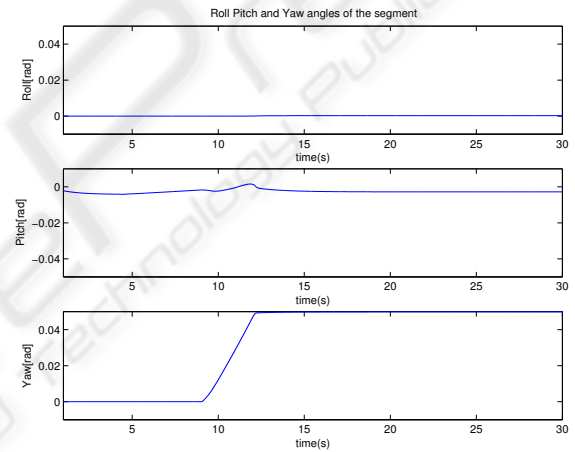


Figure 10: Orientation of the segment.

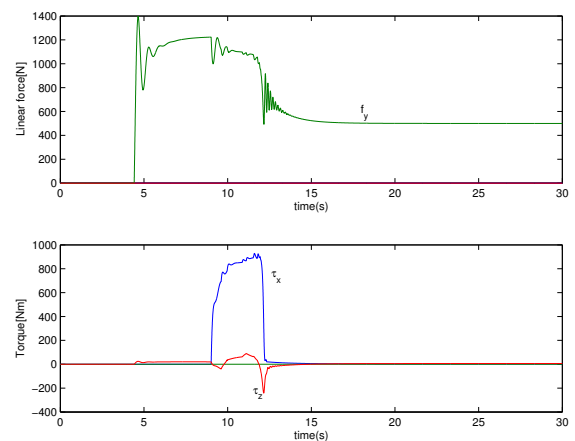


Figure 11: Force measurement in the segment force sensor (one simulation run).

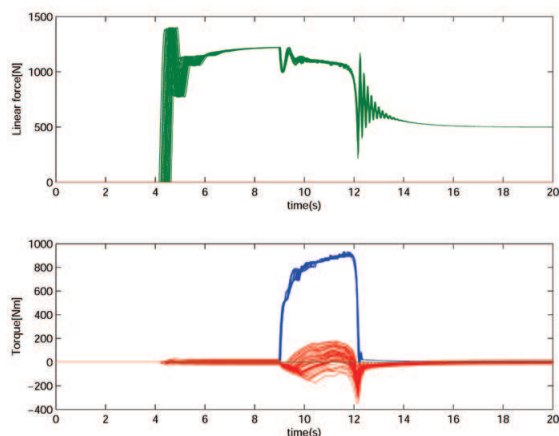


Figure 12: Force measurement in the segment force sensor (50 simulation runs).

been met by using a combination of a force controller, an impedance controller and a position controller. The position precision is 0.01 m and for the orientation the precision is 0.005 rad (0.3 degrees)

The hybrid controller is based on feedback linearization to make the system linear and decoupled. The feedback linearization is an inverse model of the manipulator. If the dynamic parameters in the feedback linearization are within 10% accuracy and the dimensional parameter are within 1% accuracy, a stable hybrid controller is obtained in simulations.

The position loops in the hybrid controller consist of a PD-controller. The P and the D gains are tuned by applying the following rules. When the natural frequency  $\omega$  and the damping ratio  $\zeta$  are known, then the P-gain is defined by  $\omega^2$  and the D-gain is defined by  $2\zeta\omega$ .

It is assumed that the manipulator head is equipped with a six DOF force sensor. If this is not possible in the mechanical design, the possibility must be investigated of estimating the force, by measuring the pressures in the hydraulic actuators.

## REFERENCES

- Hogan, N. (1985). Impedance control: An approach to manipulation: Part i - theory, part ii - implementation, part iii - applications. *ASME Journal of Dynamic Systems, Measurement, and Control*, 107:1–24.
- K. Kosuge et al. (1996). Assembly of segments for shield tunnel excavation system using task-oriented force control of parallel link mechanism. *IEEE*.
- Raibert, M. and Craig, J. (1981). Hybrid position/force control of manipulators. *J of Dyn Sys, Meas, and Cont.*
- Siciliano, B. and Villani, L. (1999). *Robot Force Control*. Kluwer Academic Publishers.

Spong, M. W. and Vidyasagar, M. (1989). *Robot Dynamics and Control*. John Wiley & Sons.

Tanaka, Y. (1995). Automatic segment assembly robot for shield tunneling machine. *Microcomputers in Civil Engineering*, 10:325–337.

Vukobratović, M. (1994). Contact control concepts in manipulation robotics-an overview. In *IEEE Transactions on industrial electronics*, vol. 41, no. 1, pages 12–24.

Zhang, H., Zhen, Z., Wei, Q., and Chang, W. (2001). The position/ force control with self-adjusting select-matrix for robot manipulators. In *Proceedings of the 2001 IEEE International Conference on Robotics & Automation*. Department of Automatic Control, National University of Defense Technology.